The role of Coulomb screening in quasi one-dimensional conductors

S. Barišić

J. Physique **44** (1983) 185-199 FÉVRIER **1983,** PAGE 185

Classification
Physics Abstracts
61.65 — 72.15N — 74.10 — 75.25

The role of Coulomb screening in quasi one-dimensional conductors

S. Barišić

Department of Physics, Faculty of Science, P.O.Box 162, 41000 Zagreb, Croatia, Yugoslavia

(*Reçu le 25 juin 1982, accepté le 13 octobre 1982*)

Résumé. — Nous considérons les électrons de conduction d'un système de chaînes avec les paramètres de réseau $d_{\|}$ et $d_{\perp}$. Les électrons sont supposés interagir par les forces de Coulomb de longue portée. Le problème est traité par l'approximation de parquet en supposant petit le rapport v de l'interaction de Coulomb entre les premiers voisins $e^2/d_{\|}$ et la largeur de bande. Les diagrammes de parquet sont calculés en utilisant l'interaction de Coulomb, écrantée non logarithmiquement, pour la diffusion vers l'avant, et l'interaction de Coulomb, nue, pour la diffusion vers l'arrière. La diffusion arrière interchaîne est supposée négligeable. L'approximation de parquet élimine alors la diffusion vers l'avant, interchaîne, écrantée. La tri-dimensionalité entre dans les résultats par écrantage de la diffusion intrachaîne vers l'avant. Cet écrantage est faible pour les chaînes écartées $d_{\perp} \gg d_{\|}$. La fonction de corrélation des ondes de densité à $2\,k_F$, calculée pour le modèle de Tomonaga, présente alors une loi en puissance dont la puissance même est logarithmiquement singulière. Lorsque les chaînes sont rapprochées, l'écrantage dynamique devient important, et les lois en puissance habituelles sont retrouvées. Toutefois, la contribution coulombienne à g_2 est augmentée logarithmiquement par rapport à l'interaction v entre les premiers voisins, soit $v \log d_{\perp}^2/v d_{\|}^2$. Les forces à grande distance favorisent donc la formation des ondes de densité à $2\,k_F$. L'effet est le plus faible lorsque les chaînes sont rapprochées, et l'on peut atteindre un régime supraconducteur à l'aide des phonons.

Abstract. — The electrons of the system of conducting linear chains with lattice parameters $d_{\|}$ and $d_{\perp}$ are assumed to interact through the long-range Coulomb forces. Assuming further that the ratio v of the first-neighbour Coulomb interaction $e^2/d_{\|}$ to the band-width is small, the problem is treated in the parquet approximation. The parquet diagrams are evaluated using the non-logarithmically screened Coulomb interaction for the forward scattering and the bare Coulomb interaction for the backward scattering. The weak interchain backward scattering is neglected. The parquet approximation eliminates then the screened interchain forward scattering. The three-dimensionality enters the results through the screening of the on-chain forward interaction. This screening is inefficient in the loosely packed chains $d_{\perp} \gg d_{\|}$. The $2\,k_F$-CDW correlation function of the corresponding Tomonaga model shows then a power law singularity with a power which itself is logarithmically singular. In the closely packed chains the important screening is dynamic. It is very efficient and the usual power laws are recovered. The Coulomb contribution to g_2 is however logarithmically enhanced with respect to the first-neighbour interaction v, i.e. it is equal to $v \log d_{\perp}^2/v d_{\|}^2$. The long-range forces thus enhance the tendency to the formation of the $2\,k_F$-CDW or SDW. In the closely packed chains the effect is weakest and with the help of phonons the superconducting regime can be attained.

1. **Introduction.** — The recent discovery [1] of superconductivity in some organic metals has renewed interest in the origin of this phase. Particularly indicative in this respect is the phase boundary between the superconducting phase and the spin or charge density wave phase, which was observed on applying pressure to these materials. Indeed, in the conventional (three-dimensional) conductors the spin density phase is associated with the strong repulsion and therefore cannot continuously turn into the BCS phase.

It was realized a long time ago that such phase boundaries can occur in (quasi) one-dimensional conductors, due to the one-dimensional logarithmic singularity in the electron-hole channel, additional to the logarithmic singularity in the electron-electron channel which is independent of the dimension. The first consistent many-body theory of this effect was formulated [2] for the weak-coupling band model. It represented one of the first applications of the method of parquet summation required when two channels are singular. The weak-coupling theory (band model) was subsequently completed [3, 4] by the inclusion of the Umklapp terms, spin-orbit couplings, interchain electron-electron interactions, interchain hopping and terms beyond the parquet approximation. In particular, the

study [3, 5] of interchain hopping led to the better understanding of the role of some early [6] « mean-field » (ladder) theories [7] for quasi one-dimensional materials. The common feature of all these theories is that they are based on the short-range extensions of the Hubbard Hamiltonian. We shall call them constant-interaction theories, because in the reciprocal space the interaction is a slow function of the wave-vector $q_{\|}$. Using the results of these theories it was possible to understand [8-10] the phase diagram of many novel chain-materials in terms of three interaction constants, the backward ($q_{\|} \simeq 2\,k_F$) scattering g_1, the forward ($q_{\|} \simeq 0$) scattering g_2 and the small Umklapp scattering g_3. It turned out that although this latter constant controls the phase diagram of the organic superconductors at very low temperatures, most of the basic physics is contained in the combination $g_2 - \frac{g_1}{2}$, or even better, in its sign. E.g. in the absence of g_3, $g_2 - \frac{g_1}{2} > 0$ is associated [3, 4] with density waves and $g_2 - \frac{g_1}{2} < 0$ with superconducting fluctuations.

Not much is known about $g_2 - \frac{g_1}{2}$. It is not even clear that it is legitimate to use this quantity in chain conductors. $g_2 - \frac{g_1}{2}$ contains the forward scattering g_2, and the difference between g_1 and g_2 is attributed to the already mentioned short-range interactions ($g_1 = g_2$ in the Hubbard model). On the other hand it was pointed out a long time ago [11] that even in the tight-binding limit, which is appropriate to all known chain conductors, the electrons interact *via* long-range Coulomb forces. The corresponding bare forward interaction is by no means a constant — it contains the Coulomb singularity. Moreover, the measurements [12] of the plasma frequency ω_0 have shown that the strength of the Coulomb singularity is not particularly small in the existing materials : ω_0 is comparable to the Fermi energy ε_F. At the same time the observation of the intraband plasmons suggests that the metallic screening of the forward interaction may be important. The interesting question which we shall address here is whether and under which conditions is the forward scattering screened enough to became comparable to the backward scattering, allowing for the transition between the density wave and superconducting regimes.

Previously, the role of the Coulomb singularity was only briefly discussed within the Tomonaga model [13]. This included the evaluation of the electron propagators, but the correlation functions were not found. The purpose of the present paper is to determine these correlation functions, not only for the Tomonaga model but also including the physically important backward scattering. We chose to do it within the parquet approximation, i.e. in the weak-coupling limit. The advantage of the parquet approximation is that from the outset it treats the forward and the backward scattering on equal footing and that it can be rather easily extended to various physically interesting situations.

The paper is organized as follows : in section 2 we review the main facts concerning the screening of the long-range forces in the quasi one-dimensional conductors. Parquet approximation is briefly discussed in section 3, emphasizing the properties important for the evaluation of the parquet sum when the dynamically screened Coulomb force replaces the usual constant g_2. Section 4 deals with the elementary parquet diagrams. Some questions are more easily discussed in terms of second-order parquet diagrams of section 5, where also the required general properties of the parquet diagrams are verified. In section 6 we find the $2\,k_F$-CDW correlation function of the Tomonaga model in the extreme weak-coupling limit for the Coulomb forces. Section 7 is devoted to the qualitative study of the corrections to the weak-coupling results when the intermediate couplings are approached, with the emphasis on the ladder diagrams. Some effects of the backward scattering are discussed in the last section which also summarizes the results.

2. **Model.** — In this section we wish to construct the simple model which includes the effects of the long-range Coulomb electron-electron interaction. Also, we shall briefly review what is known about the non-logarithmic screening of these long-range forces. Let us thus consider the square lattice of the equivalent, parallel chains at distance $d_{\perp}$, assumed larger than the intersite distances within the chain $d_{\|}$. The electrons are allowed to move along the chains with the Fermi velocity v_F, i.e. we here neglect the interchain hopping and linearize the electron spectrum around the Fermi level ε_F. This is legitimate in the weak-coupling limit, the meaning of which will become clear in the course of our discussion.

The Coulomb interaction between electrons at large distances is correctly described by the point-charge approximation, even when the electron sites are extended as is for example the case in organic metals. The corresponding behaviour of the Coulomb

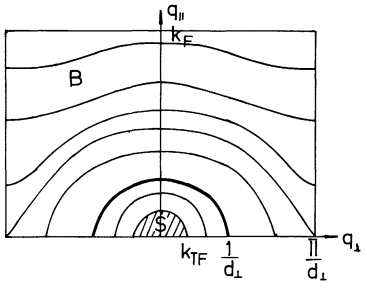

Fig. 1. — Behaviour of Coulomb matrix element v in reciprocal space. B and S denote bare and screened regions, respectively.

matrix element $u + v\alpha$ in the reciprocal space spanned by the vectors $\mathbf{g}$ is illustrated in figure 1. Here $u = n_F U$, $v = \frac{n_F e^2}{d_\parallel}$, where $n_F = \frac{d_\parallel}{2\pi v_F}$ and U, $e^2/d_\parallel$, denote respectively the on-site and the first-neighbour Coulomb interactions. α is the Madelung constant

$$\alpha = \sum_{\mathbf{g}} \frac{4\pi}{d_\perp^2 (\mathbf{q} + \mathbf{g})^2} . \tag{1}$$

From equation (1) we see that the matrix element $u + v\alpha$ shows the three-dimensional behaviour

$$\alpha \simeq \frac{4\pi}{d_\perp^2 \mathbf{q}^2} \tag{2}$$

for $|\mathbf{q}| < d_\perp^{-1}$, as is also seen in figure 1 which illustrates further how this behaviour crosses over [14] into the one-dimensional regime. The weak transverse dispersion, occurring in figure 1 for $q_\parallel > d_\perp^{-1}$ arises from the weak interchain scattering, proportional to $\exp(- q_\parallel d_\perp)$ in the point-charge approximation. As usual [3], we shall divide the scattering in the forward and backward parts, $|q_\parallel| < k_F$ and $|q_\parallel \pm 2k_F| < k_F$ respectively. On physical grounds we shall assume

$$k_F \approx \frac{1}{d_\parallel} > \frac{1}{d_\perp} . \tag{3}$$

In this way the strong Coulomb singularity (2) falls in the forward region, while in the backward region both the on-chain term g_1 and the interchain term $g_1^\perp$ can be considered as the non-singular functions of $q_\parallel$. The latter can be thus set equal to $2k_F$ and we get from equation (1), [14] :

$$\begin{aligned} g_1 &= g_1^\parallel + g_1^\perp \\ g_1^\parallel &\approx u - v \log 2(1 - \cos 2k_F d_\parallel) \\ g_1^\perp &\approx v \frac{e^{-2k_F d_\perp}}{\sqrt{2k_F d_\perp}} (\cos q_\perp d_\perp)_{1,2} . \end{aligned} \tag{4}$$

The condition (3) making g_1 a non-singular function of $q_\parallel$ uses the point-charge approximation in the range of its validity. However, this approximation breaks around $q_\parallel = \frac{\pi}{d_\parallel}$, $q_\perp = \frac{\pi}{d_\perp}$ in materials with large molecules and then equations (4) are merely an indication that $g_1^\parallel \gg g_1^\perp$. Indeed it has been shown [15] that this relation remains valid in the more elaborate models. Focusing our attention on the role of the forward Coulomb singularity we shall thus neglect $g_1^\perp$ in the following.

In the next section we shall see that in the absence of $g_1^\perp$ the forward scattering gets integrated over $q_\perp$ in all correlation functions of interest, which are thus determined only by the on-chain forward term. The forward on-chain term corresponding to equations (1) and (2) is

$$u + 2v \log \frac{\varepsilon_F}{|\xi|} , \tag{5}$$

where we have used equation (3), defined the Fermi energy by $\varepsilon_F = v_F k_F$, and set $\xi = v_F q_\parallel$. We note that (5) is logarithmically singular. Obviously, such singularity requires a full care in the theory which is logarithmic by itself. We shall proceed therefore by first introducing the non-logarithmic screening of the strongest singularity in the problem, namely the Coulomb singularity (2). In the next step, we shall deal with the problem of logarithmic singularities through the parquet diagrams evaluated with the non-logarithmically screened Coulomb interaction.

This programme can be carried out by using the dielectric constant ε calculated either in the RPA [16] or in the Tomonaga model [13]. Let us therefore review briefly the properties of this quantity. The RPA dielectric constant contains two nearly coalescent logarithmic singularities at $\omega \approx \xi$, ($\xi = v_F q_\parallel$) but they are inessential since they average out in the integral properties, and the diagram calculations involve integrals over frequencies and momenta. Therefore we shall use the simpler expression for the dielectric constant. Anticipating that we shall need it on the imaginary axis $\omega = i\eta$ we put [13]

$$\varepsilon^{-1} = \frac{\eta^2 + \xi^2}{\eta^2 + \omega_p^2} ; \tag{6}$$

where $\omega_p^2 = [1 + 4(u + v\alpha)] \xi^2$ is the anisotropic plasma frequency.

Let us first consider the static limit of (6), $\eta < \xi$. Ignoring $u < 1$ we see that the screening is important in the range $4v\alpha > 1$. Assuming further that v is small compared to unity the solution of the equation $4v\alpha = 1$ falls into the three-dimensional regime (2) of figure 1 and defines the screening wave-vector k_{TF} by

$$k_{TF}^2 d_\perp^2 = 16\pi v < 1 . \tag{7}$$

The weak-coupling limit thus necessarily implies that the screened range of the Brillouin zone (Fig. 1) is three-dimensional. For $|\mathbf{q}| < k_{TF}$ we find the usual Thomas-Fermi three-dimensional static screening, whereas for $|\mathbf{q}| > k_{TF}$ the screening disappears.

The plasma frequency plays a role in the frequency scale analogous to the one k_{TF} plays in the momentum space. Equations (2) and (6) give

$$\omega_p^2 \approx \omega_0^2 \frac{q_\parallel^2}{q_\parallel^2 + q_\perp^2} \quad \text{for} \quad |\mathbf{q}| < k_{TF} \tag{8}$$

i.e. when $4v\alpha > 1$. The screening is dynamic for $\omega_p > \omega > \xi$ and disappears for $\omega > \omega_p$. The maximum plasma frequency (Coulomb energy scale) ω_0 is related to k_{TF} (Coulomb momentum scale) by ($\hbar = 1$)

$$\omega_0 = v_F k_{TF} . \tag{9}$$

In summary, the Coulomb screening, static or dynamic, is efficient for

$$v_F |\mathbf{q}| , \quad \eta < \omega_0 . \tag{10}$$

Outside this region the screening is, roughly speaking negligible, $\varepsilon \approx 1$. This completes our digression on the properties of the dielectric constant and we can now evaluate the screened on-chain forward scattering which is to replace equation (5) in parquet calculations.

The averaging of $[u + v\alpha]\ \varepsilon^{-1}$ over the transverse Brillouin zone can be performed only approximately in spite of the existence of the closed expressions (1) and (6). In agreement with the condition (10) we shall consider separately the two regions $q_\perp^2 \gtrless k_{TF}^2 - q_\parallel^2$ for $q_\parallel^2 < k_{TF}^2\ (\xi < \omega_0)$ and evaluate the contribution of each region to the on-chain forward scattering. In the screened range $q_\perp^2 < k_{TF}^2 - q_\parallel^2\ (\xi < \omega_0)$ u is negligible and we shall use the approximate expressions (2) and (8) to calculate the contribution v_s of this range to the on-chain interaction,

$$v_s = \frac{d_\perp^2}{4\pi} \int_0^{k_{TF}^2 - q_\parallel^2} dq_\perp^2 \frac{4\pi v}{\mathbf{q}^2 d_\perp^2}\, \varepsilon^{-1} = \\ = 2v \int_\xi^{\omega_0} \frac{d\omega_p}{\omega_p} \frac{1}{\varepsilon}. \quad (11)$$

In (11) we used the simplicity of the approximate expression (2) for α to transform the integration over $q_\perp^2$ into the integration over ω_p, using (8). This is suitable because ε of equation (6) depends on $q_\perp$ only through ω_p. For η real the two poles of ε^{-1} do not fall on the integration axis of (11). Collecting the contributions of all three poles in (11) we thus find

$$v_s = v \frac{\eta^2 + \xi^2}{\eta^2} \log \frac{\omega_0^2}{\xi^2} \frac{\eta^2 + \xi^2}{\eta^2 + \omega_0^2}, \quad \xi < \omega_0. \quad (12)$$

In the remaining part of the Brillouin zone, $q_\perp^2 > k_{TF}^2 - q_\parallel^2$ for $q_\parallel^2 < k_{TF}^2\ (\xi < \omega_0)$ or all $q_\perp$ for $q_\parallel^2 > k_{TF}^2$, we set $\varepsilon = 1$. Accordingly, we shall call this range the bare range and calculate its contribution to the on-chain interaction by integrating $[u + v\alpha]$ over $q_\perp$ with appropriate cut-offs. It follows immediately that the contribution to the forward on-chain scattering proportional to u is

$$u_B \approx \begin{cases} u(1 - k_{TF}^2 d_\perp^2) & \xi < \omega_0 \quad (13a) \\ u & \xi > \omega_0. \quad (13b) \end{cases}$$

In the same way we find the contribution g_B of the bare range to the on-chain forward scattering, proportional to v,

$$g_B \approx \begin{cases} 2v \log \dfrac{\varepsilon_F}{\omega_0} & \xi < \omega_0 \quad (14a) \\ 2v \log \dfrac{\varepsilon_F}{|\xi|} & \xi > \omega_0. \quad (14b) \end{cases}$$

Equation (14a) follows from the observation that on adding equations (12) and (14a) valid for $\xi < \omega_0$ we must obtain for $\eta > \omega_0$ the full bare Coulomb on-chain interaction (5) or (14b), in agreement with the condition (10).

In conclusion, the screened on-chain Coulomb long-range interaction given by (12) and (14a) for ξ, $\eta < \omega_0$ goes over into the bare on-chain term (5) or (14b) when either ξ or η exceed ω_0. This is what remains of the condition (10) after the transverse integration.

3. **Parquet approximation.** — The general parquet diagram can be considered as an iteration of the first-order parquet diagrams in which two electron propagators combine in one logarithmic integration [2]. There are three types of diagrams, which appear in the parquet theory [2, 17-19]. First we have the diagrams with four external electron lines (square diagrams), the elementary representatives of which are shown in figures 2 to 5 (omitting those involving only the short-range forces g_1). Next, there are diagrams with two external electronic lines (e.g. Fig. 2 with g_1 omitted, figures 6, 7 and 10) which we shall call triangular diagrams. Finally we have the correlation function diagrams without external electron lines, such as that of figure 8. The square and the triangular vertices are the intermediate quantities in the calculation of the correlation functions.

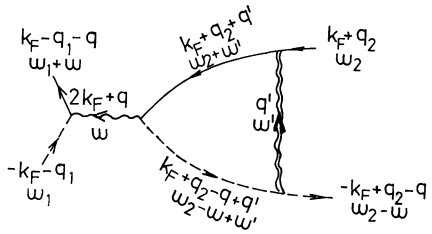

Fig. 2. — Elementary parquet e-h contribution $g_1\ M$ to the backward vertex. Full and dashed lines are electron propagators at k_F and $-k_F$ respectively, double wavy line is the forward and the wavy line the backward interaction. Transverse momenta are not exhibited (see text).

The examination of the low-order diagrams in the constant-interaction theory shows that some variables appear as natural variables of the theory. In the diagrams of the electron-hole (e-h) type (« reducible » in the e-h channel [18], by cutting two e-h lines), such as those of figures 2, 4, 6, 7 and 8, the natural variable involves the difference of the longitudinal

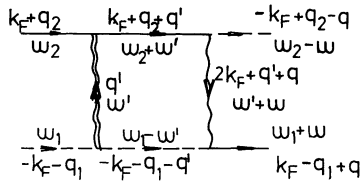

Fig. 3. — Elementary parquet e-e contribution $g_1\ C$ to the backward vertex. Notation here and in other diagrams is the same as in Fig. 2.

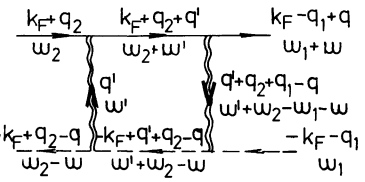

Fig. 4. — Elementary parquet e-h contribution $\tilde{B}$ to the forward vertex.

momenta (measured from $2\,k_F$) and the difference of the frequencies entering the e-h channel. In the notations of our figures these are, $q_\parallel$, ω, respectively. Likewise in the Cooper (e-e) channel the important combination is the sum of the momenta and frequencies namely $q_{2\parallel} - q_{1\parallel}$, $\omega_2 + \omega_1$. Indeed, at $T = 0$ the first-order diagrams of the constant-interaction theory are logarithmic in the natural variables, i.e. proportional to $\log \mid \max(q_\parallel, \omega) \mid$ or to $\log \mid \max(q_{2\parallel} - q_{1\parallel}, \omega_1 + \omega_2) \mid$. This result becomes particularly simple in the Matsubara diagrammatic formulation which works with imaginary frequencies. Setting

$$\begin{aligned} \Omega_i &= \xi_i + i\eta_i \\ \xi_i &= v_F\, q_{i\parallel} \\ \omega_i &= i\eta_i \end{aligned} \tag{15}$$

we see that the natural variables can be understood as the moduli of the complex energies, Ω and $\Omega_2 - \overline{\Omega}_1$ in the e-h and e-e channel, respectively. As will be also illustrated below, in the constant-interaction case the natural variables can be identified with the lower cut-offs of the logarithmic integrations. The parquet theory with constant-interactions proceeds further by proving that these properties can be generalized to the vertices of the arbitrary order. E.g. the vertices of the e-h type depend only on $\mid \Omega \mid$ when the latter is the largest variable, the same role being kept by $\mid \Omega_2 - \overline{\Omega}_1 \mid$ in the e-e channel. Furthermore it is possible to identify the natural variables in the respective channels with the cut-off energies for the logarithmic integrations in those channels. This turns out to be of great practical importance. Using the identification of the natural variables with the cut-off energies it is possible to reformulate the theory [2, 17, 18] so that the important values of the natural variables in both channels are of the same order of magnitude. Further steps can thus be performed in terms of the unique variable $\mid \Omega \mid \approx \mid \Omega_2 - \overline{\Omega}_1 \mid$.

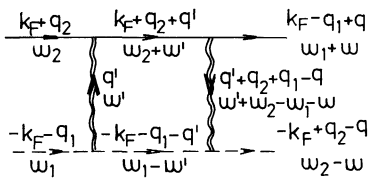

Fig. 5. — Elementary parquet e-e contribution $\tilde{C}$ to the forward vertex.

This simplifies considerably the integral equations for the renormalized vertices (Sudakov theory), and, by the appropriate use of the single variable triangular vertices, allows [17] the determination of the correlation functions. It can be added that the integral equations of the single variable theory can be cast [19] in the differential form, which turns out to be identical to the first-order renormalization group Lie equations [3, 4]. This shows that the homogeneity assumptions [3] behind the Lie equations are correct at least to the considered order.

In summary, the vertex properties required for the transformation to the single variable theory are :

(i) that the vertex depends only on its natural variable when the latter is the largest;

(ii) that the natural variable can be identified with the cut-off energy for logarithmic integrations in the considered channel.

Although derived in the constant-interaction case these properties concern the general vertices and therefore need not be related to the use of constant-interactions. Indeed in the forthcoming sections we shall show that under certain conditions the single variable theory continues to hold with our long-range interactions, but gives results quite different from those obtained in the constant-interaction case. It will appear that the single variable theory breaks through the condition (ii) and we shall examine some consequences of this breakdown. However, before turning to the actual evaluation of the parquet diagrams with long-range forward scattering, we wish to argue that in absence of $g_1^\perp$ we can use only its on-chain component, as was already anticipated in the preceding section.

An exact argument shows [20] that the forward interchain scattering alone cannot order the correlation functions ($2\,k_F$-CDW). The parquet approximation satisfies this general requirement in a simple way : in the absence of $g_1^\perp$ all the triangular (and thus the correlation function) diagrams involve only the on-chain forward interaction. In other words, the parquet theory is effectively one-dimensional in the absence of $g_1^\perp$. This can be readily seen by first assuming that the forward interaction depends on the relative distance between the chains, i.e. that it is periodic in the transfer of the transverse momentum. Then the transverse integrations of the forward interactions over the whole transverse zone of periodicity reduce the interactions to the on-chain terms. Not suprisingly, this result known in the parquet theory with short-range forces [19, 21] remains valid irrespective of the dependence of the forward scattering on the longitudinal momentum.

The conclusion is of practical importance in the evaluation of the square vertices. Let us illustrate this point on the low-order diagrams. The on-chain forward scattering appears naturally, by a transverse integration, in figure 2 and also in figure 3 when

$g_1^{\perp} = 0$. However this is not so with figures 4 and 5. In the two latter cases there is only one transverse integration for the two forward interactions, i.e. the usual diagram rules leave these diagrams with a complicated transverse wave-vector structure. Only the additional transverse integration in the triangular diagrams of figures 6 and 7, generated by the square diagrams under consideration, reduces both interactions to the on-chain terms. Since the final result is independent of the inter-chain forward scattering we can use the on-chain forward interaction from the outset, i.e. even in the intermediate square vertices. (This is why the transverse wave-vectors are not shown in our figures.)

In fact it would be interesting to know whether or when the single variable theory holds for finite $g_1^{\perp}$. However, this problem requires the investigation of the interference effects between the forward and backward interchain scatterings, which is beyond the scope of the present paper.

4. **First-order diagrams.** — In this section we shall consider the elementary parquet square diagrams. There are four representatives of this kind, omitting those which do not involve the forward scatterings and thus do not bring anything new. The diagrams in figures 2 and 3 contribute to the backward scattering and those in figures 4 and 5 to the forward scattering.

Let us first consider the backward scatterings shown in figures 2 and 3 because they are somewhat simpler than the forward terms of figures 4 and 5. g_1 in figures 2 and 3 is not involved in the integration and we can conveniently write the contribution of these figures as $g_1\, M(\bar{\Omega}_2,\ \Omega - \Omega_2)$ and $g_1\, C(\bar{\Omega}_2, \bar{\Omega}_1)$ respectively, using the Matsubara notations of equation (15). M and C are the first-order triangular vertices and from figures 2 and 3 we find by observation

$$C(\bar{\Omega}_2, \bar{\Omega}_1) = - M(\bar{\Omega}_2, - \bar{\Omega}_1)\,. \tag{16}$$

This relation allows us to determine C once M is known. It also shows that in the quasi one-dimensional case $g_1 \approx g_1^{\parallel}$ the square vertex contributions $g_1\, M$ and $g_1\, C$ cancel for $\Omega_2 - \bar{\Omega}_1 = \Omega$. This cancellation is however useful only if the special values $\Omega_2 - \bar{\Omega}_1 = \Omega$ of the external variable are of particular importance. Indeed, in $| \Omega_2 - \bar{\Omega}_1 |$ and $| \Omega |$ we recognize the natural variables of section 3 and the values $| \Omega_2 - \bar{\Omega}_1 | \approx | \Omega |$ carry the single variable parquet theory, provided that the latter is valid, i.e. the conditions (i) and (ii) of section 3 fulfilled. Then the cancellation of $g_1\, M$ and $g_1\, C$ extends to all orders of the single variable theory and leads to simplifications.

Let us thus start examining M from this point of view. There are three contributions to M, M_S, M_u and M_B corresponding to the contributions (12), (13) and (14) to the on-chain forward scattering respectively. The simplest is M_u,

$$M_u = \frac{1}{2\pi} \int_{-\varepsilon_F}^{\varepsilon_F} \int_{-\infty}^{\infty} \frac{d\xi'\, d\eta'\, u_B}{(\bar{\Omega}' + \bar{\Omega}_2)(\Omega' + \Omega_2 - \Omega)}, \tag{17}$$

where, for simplicity we have taken the $T = 0$ limit of the Matsubara formulation (15) i.e. replaced the summation over the imaginary frequencies by the integration over η'. For small external frequencies u_B in (17) can be taken as given by (13*a*) because only the small values of energies matter. The result for M with constant-interaction is well known,

$$M_u = u_B \log \frac{\varepsilon_F}{| \Omega |}, \tag{18}$$

but it is instructive to see how it arises in our formulation. Keeping in mind $| \Omega |$ in (18) we pass to the polar variables ρ', ϕ' in (17). It can be easily seen that the integration stripe along the η' axis of the width $2\,\varepsilon_F$ can be replaced to a good approximation by the circle of radius ε_F. The ϕ'-integration in (17) results in two contributions to the ρ'-integral which can be contracted into one using the fact that the interaction is constant. The lower cut-off of this logarithmic integration is determined by $| \Omega |$ while Ω_2 is negligible since small with respect to ε_F. In other words in (17) we can neglect Ω_2 and « ignore » the angular integration on transferring Ω from the denominator of the integrand to the lower limit of the radial integration, to get the result (18). From this consideration it also follows immediately that u_B of equation (13*a*), which figures in (18) for $| \Omega | < \omega_0$, is to be replaced by u of (13*b*) for $| \Omega | > \omega_0$. This shows in detail how $g_1\, M_u$ satisfies the conditions (i) and (ii) of section 3.

M_S and M_B differ from M_u by the fact that the corresponding interactions (12) and (14), which replace u_B in (17) are logarithmic rather than constant. We shall show now that the logarithmic dependence on ϕ' can remove $| \Omega |$ from the lower limit of the logarithmic ρ'-integration, contrary to the logarithmic dependence on ρ'.

The logarithmic dependence on ϕ' appears in M_S. Indeed, for $\eta < \omega_0$, v_s of equation (12) can be cast in the form

$$v_s(\phi') = \frac{v}{\sin^2 \phi'} \log (1 + \tan^2 \phi')\,. \tag{19}$$

The only singularity in (19) occurs for $\phi' = \frac{\pi}{2}$ ($\eta' \gg \xi'$). On the other hand the product of the electron propagators is weakly dependent on ϕ', and we can set $\phi' \approx \pm \frac{\pi}{2}$ in this part of the expression for M_S. Then the angular integration involves only the interaction (19)

$$g_S = \frac{1}{\pi} \int_0^{\pi} v_s(\phi')\, d\phi' = 2\, v\,. \tag{20}$$

which factorizes out in M_S. The remaining radial integration is easily performed by separating the two poles in the product of the propagators. In this way we find the singular part of M_S as

$$M_S = g_S \frac{1}{\Omega_2 - \Omega + \bar{\Omega}_2}\left[(\Omega_2 - \Omega)\log\frac{\omega_0}{|\Omega_2 - \Omega|} + \bar{\Omega}_2 \log\frac{\omega_0}{|\Omega_2|}\right]$$
$$\approx g_S \log \omega_0/\max(|\Omega|, |\Omega_2|). \tag{21}$$

We note that there is no singularity at $\Omega_2 - \Omega + \bar{\Omega}_2 = 0$. The strong anisotropy of $v_s(\phi')$ has therefore important consequences. First, it separates the logarithmic singularity of the interaction, in ϕ', from the logarithmic singularity of the propagators in ρ'. Thus the former singularity can be integrated out in equation (20), making M_S logarithmic in the external variables, similarly to M_u. Second, unlike M_u, M_S depends on $|\Omega_2|$. This may seem unimportant because (21) satisfies the condition (i) of section 3. However the appearence of Ω_2 in (21) is also related to the breakdown of the condition (ii). So the third consequence of the anisotropy in v_s is the departure of M_S from the requirements of the single variable parquet theory. Indeed, $|\Omega|$ does not act as a cut-off energy in equation (21) : omitting Ω in the radial integrand by introducing $|\Omega|$ into the lower limit of the radial integration leads to the result different from (21).

Let us now evaluate M_B, the contribution to M corresponding to g_B of equation (14). For $\xi > \omega_0$ the interaction g_B becomes anisotropic. However,

$$\log|\xi'| = \log\rho' + \log|\cos\phi'| \tag{22}$$

shows that g_B contains the radial component. The leading singularity in M_B comes just from the coupling of this component with the ρ'^{-1} singularity in the electron propagators. In this contribution to M_B the ϕ'-integration is the same as in M_u. In contrast to M_u, here the interaction is not a constant but a logarithmic function of ρ' for $\rho' > \omega_0$ (power of log in higher-order diagrams). However this logarithmic behaviour is sufficiently slow to leave $|\Omega|$ in the lower limit of the ρ'-integration, (as in the higher-order diagrams of the constant-interaction parquet theory). Thus we find

$$M_B \approx \begin{cases} 2v\left[\log\frac{\varepsilon_F}{\omega_0}\log\frac{\varepsilon_F}{|\Omega|} - \frac{1}{2}\log^2\frac{\varepsilon_F}{\omega_0}\right] & |\Omega| < \omega_0 \quad (23a) \\ v\log^2\frac{\varepsilon_F}{|\Omega|} & \omega_0 < |\Omega| < \varepsilon_F \quad (23b) \end{cases}$$

corresponding to equations (14*a*) and (14*b*), respectively. Here

$$\frac{\omega_0^2}{\varepsilon_F^2} \approx v\frac{d_\parallel^2}{d_\perp^2} < 1, \tag{24}$$

according to (9), (7) and (3). M_B satisfies the conditions (i) and (ii) of section 3 although the logarithmic behaviour of the interaction (14*b*) reflects itself for $\omega_0 < |\Omega| < \varepsilon_F$ in the additional power of the logarithmic singularity.

We are now in a position to draw the conclusions concerning the entire M. Assuming that $\omega_0 \ll \varepsilon_F$, $g_B/g_S = \log \varepsilon_F/\omega_0 > 1$ and we can neglect M_S with respect to M_B, which itself presents two distinctive regimes $|\Omega| \gtrless \omega_0$. We shall call this limit the weak-coupling limit, although $\omega_0 \ll \varepsilon_F$ can arise either from $v \ll 1$ or from $d_\perp \gg d_\parallel$, according to (24). If we now let v and $d_\parallel/d_\perp$ simultaneously tend to unity, ω_0 tends to ε_F from below. In this intermediate coupling limit $\log \varepsilon_F/\omega_0 \approx 1$ cannot be considered as large and M_S becomes comparable to M_B. Thus, although M becomes linear in the logarithm in the whole range of interest $|\Omega| < \omega_0 \lesssim \varepsilon_F$, the single variable theory breaks down.

In summary, we have seen that the triangular vertices M and C and the square vertices $g_1 M$ and $g_1 C$ satisfy the requirements of the single variable parquet theory provided that $\omega_0 \ll \varepsilon_F$ but not for $\omega_0 \lesssim \varepsilon_F$, when, however, all these quantities become linear in the logarithms. The basic quantities of our discussion appeared to be the triangular vertices M and C, which involve only the forward scattering and are thus common to the Tomonaga ($g_1 = 0$) and the backward scattering ($g_1 \neq 0$) models : the properties of the Tomonaga model come naturally into the focus of our attention when we are dealing with long-range forces.

The square vertices $\tilde{B}$ and $\tilde{C}$, shown in figures 4 and 5 respectively, involve only the forward scattering and thus belong in the first place to the Tomonaga model. At first sight $\tilde{B}$ and $\tilde{C}$ depend on many variables in a

complicated way, because both interactions are screened. The first important simplification occurred however when we realized that even in these diagrams we can use the on-chain component only of the forward scattering. This eliminates the transverse wave-vector dependence. Concerning the dependence on the external energies we note that, in contrast to M and C, $\tilde{B}$ and $\tilde{C}$ depend on all three energies $\tilde{B}=\tilde{B}(\overline{\Omega}_2, \Omega_2-\Omega, \Omega_2-\Omega+\overline{\Omega}_1)$ and $\tilde{C}=\tilde{C}(\overline{\Omega}_2, \overline{\Omega}_1, \Omega_2-\Omega+\overline{\Omega}_1)$, so that

$$\tilde{B}(\overline{\Omega}_2, \Omega_2-\Omega, \Omega_2-\Omega+\overline{\Omega}_1) = \\ = -\tilde{C}(\overline{\Omega}_2, \Omega_2-\Omega, \Omega_2-\Omega+\overline{\Omega}_1), \quad (25)$$

instead of equation (16). For brevity we write here the « third » variable as a complex energy, although $\tilde{B}$ and $\tilde{C}$ depend on its real and imaginary parts separately, according to equations (19) and (22).

Our further aim is to examine whether $\tilde{B}$ and $\tilde{C}$ have the properties consistent with the single variable parquet theory. Focusing our attention on the anomalous contributions (12) and (14*b*) to the forward scattering, we shall show that this is the case in the weak-coupling limit $\omega_0 \ll \varepsilon_F$. In this limit the contribution of the screened range (which already produced the anomalous term M_S in M) is negligible. This can be seen from $\tilde{B}$ and $\tilde{C}$ directly, but also more easily from the triangular diagrams generated by $\tilde{B}$ and $\tilde{C}$ and discussed in the next section. Postponing to this section the proof that only the bare range matters in the $\omega_0 \ll \varepsilon_F$ limit, let us now consider the contributions $\tilde{B}_B$ and $\tilde{C}_B$ of this range to $\tilde{B}$ and $\tilde{C}$, respectively. In the next section we shall also see that the triangular diagrams generated by $\tilde{B}_B$ and $\tilde{C}_B$ are dominated by the isotropic part (22) of the interaction (14*b*) and now we shall retain only this component in $\tilde{B}_B$ and $\tilde{C}_B$. The latter then satisfy (25) as it is written, namely $\tilde{B}_B$ or $\tilde{C}_B$ are symmetric in the real and imaginary parts of the third variable. The integration in $\tilde{B}_B$ or $\tilde{C}_B$ can be performed either in the polar or in the original ξ', η' variables. Actually, it is somewhat simpler to use the latter, together with the anisotropic interactions (14*b*) and the external η's set equal to zero. Symmetrizing the result at the end we obtain

$$\tilde{C}_B = \begin{cases} 4v^2 \log^2 \dfrac{\varepsilon_F}{\omega_0} \log \dfrac{\varepsilon_F}{|\Omega_2 - \overline{\Omega}_1|} & \omega_0 > |\Omega_1, \Omega_2, \Omega| \quad (26a) \\ 2v^2 \log^2 \dfrac{\varepsilon_F}{|\Omega_2 - \overline{\Omega}_1|} \log \dfrac{\varepsilon_F}{|\Omega|} & |\Omega| > |\Omega_2 - \overline{\Omega}_1| > \omega_0, |\overline{\Omega}_1 + \Omega_2| \quad (26b) \\ \dfrac{4v^2}{3} \log^3 \dfrac{\varepsilon_F}{|\Omega_2 - \overline{\Omega}_1|} & |\Omega_2 - \overline{\Omega}_1| > \omega_0, |\overline{\Omega}_1 + \Omega_2, \Omega|. \quad (26c) \end{cases}$$

Indeed, $\tilde{C}_B$ has all the required properties. As can be seen easily, $\Omega_2 - \overline{\Omega}_1$ acts as a cut-off energy in the actual integration. Consequently, in all regimes for $\tilde{C}_B$, $\Omega_2 - \overline{\Omega}_1$ appears in the argument of at least one logarithm. However, all regimes are not important because the variable of the « third » channel, $\Omega_2 + \overline{\Omega}_1$, can be considered as small in all parquet calculations [3]. Equations (26*a*) and (26*c*) show that C_B depends only on the total energy in the Cooper channel when it is the largest among the three external energies. (26*b*) shows that when $|\Omega| > |\Omega_2 - \overline{\Omega}_1|$ C_B depends on $\log|\Omega|$ linearly, the other two logarithms being cut-off by $|\Omega_2 - \overline{\Omega}_1|$.

In contrast to that, $\Omega_2 - \overline{\Omega}_1$ looses its meaning of the cut-off energy when the contribution of the screened range is included in the intermediate coupling limit $\omega_0 \lesssim \varepsilon_F$. Accordingly, when $|\Omega|$ is large the results are no longer linear in $\log|\Omega|$, as will be discussed in the next section by comparing the contributions of the bare and screened ranges in the response diagrams generated by $\tilde{B}$ and $\tilde{C}$.

We can thus conclude that although equations (16) and (25) ensure the (near) cancellation of the vertex corrections for comparable values of the energies in the two channels and for the arbitrary values of the on-chain couplings, this cancellation is meaningful only in the weak-coupling limit $\omega_0 \ll \varepsilon_F$ when the vertices satisfy the requirements of the single variable theory.

5. **Second-order diagrams.** — In the study of $\tilde{B}$ and $\tilde{C}$ in the previous section we took for granted that

(*a*) the contribution of the screened range is negligible if $\omega_0 \ll \varepsilon_F$;

(*b*) the contribution of the angular part of equation (22) is negligible with respect to the radial part if $\omega_0 \ll \varepsilon_F$.

In this section we shall prove these statements by the examination of the triangular diagrams, which

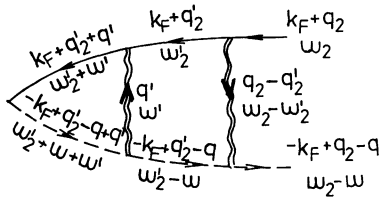

Fig. 6. — Second-order triangular ladder diagram L in the e-h channel.

can be discussed easierly in terms of the interaction variables than the square diagrams. The triangular diagrams are obtained from square diagrams by closing two external lines in the e-e (Cooper) or $2\,k_F$ e-h integration. Hence from each $\tilde{B}$ or $\tilde{C}$ we obtain one ladder diagram and one mixed diagram. If both diagrams generated by $\tilde{B}$ satisfy the conditions (*a*) and (*b*) we can deduce that so does $\tilde{B}$, i.e. that $B \approx B_B$ retained in equations (26). Since we know that $\tilde{B}_B$ satisfies the conditions (i) and (ii) we can conclude that (i) and (ii) hold for $\tilde{B}$ in weak-coupling limit $\omega_0 \ll \varepsilon_F$. Clearly, due to (25) the same procedure need not be repeated for $\tilde{C}$. In fact, according to this equation it is only important to consider one ladder diagram and one mixed diagram. With strong forward scattering it is somewhat more natural to consider the e-h channel where the many-body singularities occur and we choose to discuss the diagrams shown in figures 6 and 7.

Let us start with the ladder diagram L of figure 6. Integrating figure 6 from right to left requires first the evaluation of $\tilde{B}$, but in the previous section we were able to give the detailed expression (26) only for $\tilde{B}_B$. It is in fact more convenient to integrate figure 6 from left to right, using in both integrations the interaction variables associated with two interactions. Each of the two interactions is built from two one-dimensional contributions, (14) and (12), corresponding to the bare and screened Coulomb ranges respectively. Hence L can be decomposed as

$$L = L_{BB} + L_{BS} + L_{SB} + L_{SS} \tag{27}$$

according to the ranges which combine from left-to-right to give particular contributions to equation (27). The first left-to-right integration yields $M(\Omega_2', \Omega_2' - \Omega)$. This $M = M_B + M_S$ is the incoming quantity for the second integration in terms of $\Omega_2 - \Omega_2'$.

When evaluating L_{BB} we note that M_B of the first integration is independent of Ω_2'. Therefore it is not involved in the second integration and we find

$$L_{BB} = M_B^2(|\,\Omega\,|) \qquad \begin{matrix} \omega_0 \ll \varepsilon_F \\ \omega_0 \lesssim \varepsilon_F\,. \end{matrix} \tag{28}$$

The same result follows in the right-to-left direction from $\tilde{B}_B$ given by equations (26*b*) and (25), i.e. linear in $\log |\,\Omega_2'\,|$.

L_{SS} arises by combining the incoming M_S with the screened range of the second integration. The second interaction $v_s(\phi_2')$ carries the main angular dependence and we can set $\phi_2' = \pm\,\pi/2$ everywhere except in $v_s(\phi_2')$ itself. Using equation (20) we get a factor g_S from v_s, in addition to that appearing in the incoming M_S. The remaining radial integration is carried out in the way analogous to that for M_S and we get

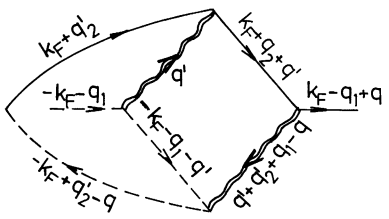

Fig. 7. — Second-order triangular mixed diagram N in the e-h channel.

$$L_{SS} \simeq \frac{1}{2\,!} g_S^2 \log^2 \omega_0/\max\,(|\,\Omega\,|, |\,\Omega_2\,|) \qquad \begin{matrix} \omega_0 \ll \varepsilon_F \\ \omega_0 \lesssim \varepsilon_F\,. \end{matrix} \tag{29}$$

The factor 1/2 ! arises from the coupling of $\log |\,\Omega_2'\,|$ in the incoming M_S with the second radial integration. According to the discussion below equation (21), $\log |\,\Omega_2'\,|$ dependence of M_S and therefore 1/2 ! is the consequence of the anisotropy of the first $v_s(\phi')$ interaction. The anisotropy of the second $v_s(\phi_2')$ interaction leads to the dependence of L_{SS} on Ω_2, i.e. to the additional factorials in the higher order terms, discussed in section 6. All these effects are not covered by the single variable parquet theory, as already discussed below equation (21).

Turning now to L_{BS} we note that the incoming M_B is independent of Ω_2'. Therefore it does not couple with the second integration, which however contains the anisotropic v_s and yields therefore M_S, which depends on Ω_2,

$$L_{BS} \simeq M_B(|\,\Omega\,|)\, M_S(\Omega_2, \Omega_2 - \Omega) \qquad \begin{matrix} \omega_0 \ll \varepsilon_F \\ \omega_0 \lesssim \varepsilon_F\,. \end{matrix} \tag{30}$$

It remains to evaluate L_{SB}. The first integration yields M_S, which couples with the radial part of the second integration. The resulting expression for L_{SB} is somewhat cumbersome if the full expression (14*a*, *b*) is used for the second interaction. For brevity we shall give only the part of the expression corresponding to g_B of (14*a*), appropriate for the intermediate couplings

$$L_{SB} \approx \frac{1}{2\,!} g_S\, g_B \log^2 \frac{\varepsilon_F}{|\,\Omega\,|} \qquad \omega_0 \lesssim \varepsilon_F\,. \tag{31}$$

However, we shall keep in mind that even the full expression for L_{SB} contains g_S as a factor.

This discussion shows that due to $g_S \ll g_B$ implied by $\omega_0 \ll \varepsilon_F$, L satisfies both conditions (*a*) and (*b*) quoted at the beginning of this section. Reading the results for L from right to left we conclude that the same is true for $\tilde{B}$ when it acts in the e-h channel. Moreover, from the factorial denominators of L_{SB} and L_{SS} we can deduce that the contributions of the screened range to $\tilde{B}$ are nonlinear in $\log | \Omega'_2 |$ when the latter is large and relate this to the fact that $| \Omega |$ looses the meaning of the cut-off frequency in these contributions to $\tilde{B}$ (Eq. (25) transfers this to $\tilde{C}$). We notice finally that all this information about $\tilde{B}$ follows from the prefactors of L, whereas the explicit frequency dependences of L (can serve to) carry the reasoning one order higher. If we now wish to investigate the behaviour of $\tilde{B}$ in the Cooper channel or of $\tilde{C}$ in the e-h channel with respect to the conditions (*a*) and (*b*) it suffices to consider the prefactors of N, analogous to those appearing in L, by ignoring the detailed dependences on the external frequencies.

The two integrations in N can be carried out in terms of the interaction variables. Dividing each integration range according to equation (10) we can write

$$N = N_{BB} + N_{BS} + N_{SB} + N_{SS} \tag{32}$$

analogously to (27). As we are not interested in the dependences on the external frequencies we can set the latter equal to zero. This simplifies considerably the product of the four electron propagators.

Assuming that the interaction is either a constant or a function of the angle, the integrations over radial variables ρ_1, ρ_2 are easily performed, as shown in the appendix. E.g. in the case of N_{SS} we get in this way

$$N_{SS} \approx -\frac{1}{\pi^2} \int_0^{\omega_0} \frac{dr}{r} \int_0^{\pi/2} \int_0^{\pi/2} \frac{\pi - 2 | \phi |}{| \sin \phi |} v_s(\phi_1)\, v_s(\phi_2)\, e^{-i\phi}\, d\phi_1\, d\phi_2\,, \tag{33}$$

where $r^2 = \rho_1^2 + \rho_2^2$ and $\phi = \phi_1 - \phi_2$. We see that the main singularities of N_{SS} come from the propagators. Indeed, the $| \sin \phi |^{-1}$ singularity occurs on the diagonal of the integration range, whereas $v(\phi_i)$ have weaker singularities on the two upper limits. These singularities weakly overlap with the main singularity, and can be integrated out. This leads to N_{SS} quadratic in the logarithms with the prefactor $-\frac{2c}{\pi} v^2$, where

$$c \approx \int_0^{\infty} dx(1 + x^2) \log^2\left(1 + \frac{1}{x^2}\right) \approx 4.2\,!. \tag{34}$$

Also, one cut-off frequency is modified to $x_0\, \omega_0$, where

$$\log x_0 \approx \frac{1}{c} \int_0^{\infty} dx(1 + x^2) \log^2\left(1 + \frac{1}{x^2}\right) \log x \approx -\frac{3\,!}{2\,!}. \tag{35}$$

Let us first consider the $\omega_0 \ll \varepsilon_F$ limit in which N_{SS} has to be compared to N_{BB} calculated with the constant-interactions (14*a*) instead of v_s in equation (33). According to (34), which is the N-analogue of (20) for M, we can again invoke the $\log \varepsilon_F/\omega_0 > 1$ argument to neglect N_{SS} with respect to N_{BB}. The similar discussion is valid for N_{SB} and N_{BS}. This proves the validity of the condition (*a*). Turning now to the condition (*b*), we can continue to keep the external energies equal to zero, considering for qualitative purposes the extreme $\omega_0 \to 0$ limit. For the angular part of equation (22) we can thus use (33), with v_s replaced by $v \log | \cos \phi |$ in the integrand and ω_0 by ε_F in the limits of the integration. $v \log | \cos \phi |$ has the same singular properties as v_s. The resulting expression similar to N_{SS} has to be compared to the expression for N_{BB} in which the $v \log \rho_i$ interactions couple to ρ_i-integrations of the appendix. Thus N_{BB} is obviously more singular than its angular counterparts, as required by the condition (*b*) of this section. Hence (*a*) and (*b*) are satisfied by $\tilde{C}$ when it acts in the e-h channel. According to the discussion in the beginning of this section this completes our proof that $\tilde{B}$ and $\tilde{C}$ satisfy the conditions (i) and (ii) of section 3.

Lacking the $\log \varepsilon_F/\omega_0 > 1$ argument in the $\omega_0 \lesssim \varepsilon_F$ limit we have to worry about the numerical factors. In the case of L the angular integrations in L_{SS} and L_{BB} have introduced in L_{SS} the coupling of the radial integrations absent in L_{BB}. In contrast to that, the radial integrations in N_{SS} and N_{BB} lead to qualitatively the same angular structure of the N_{SS} and N_{BB} integrands, as already mentioned above. The anomalous factorial denominators analogous to those in L, thus do not occur in N. This is further discussed in section 7, in a somewhat more general context.

6. **Tomonaga model for $\omega_0 \ll \varepsilon_F$.** — In section 4 we have already pointed out that the basic model for the study of the long-range forces in the Tomonaga

model, which omits the short-range interactions g_1 and u. In such a model the spin does not play an explicit role and only one square vertex is involved, namely the renormalized forward scattering. In this respect the problem is analogous to the X-ray singularity problem studied in reference [18]. The analogy became even closer when we realized that our results for $\omega_0 \ll \varepsilon_F$ can be expressed in terms of the radial variables only, and that they satisfy the conditions (i) and (ii) of section 3 for the applicability of the single variable parquet theory.

However, before going to the straightforward summation of the parquet it is instructive to sum the ladder diagrams when both equations (14*a* and *b*) are used and the full expression (23*a*, *b*) for M_B is iterated into a ladder. Equation (28) shows that the ladder is geometric, $(1 - M_B)^{-1}$, but, according to (23) the nature of the expansion variable M_B changes between the low and high frequency limits. We can thus expect that if the ladder remains geometric in M_B at $|\Omega| > \omega_0$, the parquet remains exponential in this same sense.

Turning now to the parquet summation we first realize that the single variable parquet theory extends the cancellation (25) of $\tilde{B}_B$ and $\tilde{C}_B$ for $|\Omega| \approx |\Omega_2 - \overline{\Omega}_1|$ to all orders. The forward vertex remains therefore unrenormalized

$$\Gamma_2 = g_B(|\Omega|), \tag{36}$$

where $g_B(|\xi|)$ is given by (14*a*, *b*).

In our present model the $2k_F$-CDW and the $2k_F$-SDW correlation functions exibit the same singularity, and we can denote both of them by P. If we define $\tilde{P} = dP/d(\log \varepsilon_F/|\Omega|)$ the latter is the renormalized triangular vertex. As we have shown that the elementary triangular vertices satisfy the requirements of the single variable theory we can determine $\tilde{P}$ in the usual way

$$\frac{d(\log \tilde{P})}{d\left(\log \frac{\varepsilon_F}{|\Omega|}\right)} = \Gamma_2 . \tag{37}$$

Substituting (36) in (37) we find

$$\log \tilde{P} = M_B , \tag{38}$$

as anticipated above. (38) is the central result of this paper. It completes the way from equations (14) *via* (23), (25), (26), (28), (33) to the final result. This equation shows that the power of the correlation function singularity is itself logarithmically singular

$$\tilde{P} \sim |\Omega|^{-v \log \frac{\varepsilon_F}{|\Omega|}} \quad \text{for} \quad |\Omega| > \omega_0 . \tag{38a}$$

This result was first found by the bosonization method (22). (38) also shows how this behaviour crosses over into the usual power law

$$\tilde{P} \sim |\Omega|^{-2v \log \frac{\varepsilon_F}{\omega_0}} \quad \text{for} \quad |\Omega| < \omega_0 \tag{38b}$$

and gives the value of the corresponding coupling constant $g_2 = g_B$ in terms of the microscopic parameters v and $d_{\|}/d_{\perp}$ of equation (24).

The crossover between the two regimes may occur for $M_B(|\Omega| = \omega_0) \approx v \log^2 \varepsilon_F/\omega_0$ smaller or larger than unity, i.e. in the perturbative or the many-body regime, respectively. Thus, if $\log \varepsilon_F/\omega_0 > v^{-1/2}$ (loosely packed chains, $d_{\perp} \gg d_{\|}$, according to Eq. (24)), our result (38*a*) gives new many-body features due to the long-range of the Coulomb forces. If on the contrary $v^{-1/2} > \log \varepsilon_F/\omega_0 > 1$ (closely packed chains) the whole many-body singular regime is of the conventional nature. When $\log \varepsilon_F/\omega_0$ tends to unity (closely packed chains, $v \lesssim 1$) we have to start worrying about the contribution of the screened range. This contribution is further discussed in the next section.

7. **Tomonaga model — Ladder diagrams.** — In this section we shall consider the limit $v^{-1/2} > \log \varepsilon_F/\omega_0 \gtrsim 1$ when the complications with the $|\Omega| > \omega_0$ regime can be ignored, but when we have to include the contributions of the screened range on assuming $\omega_0 \lesssim \varepsilon_F$, i.e. $\log \varepsilon_F/\omega_0 \approx 1$. In other words we shall consider the corrections to the conventional constant-interaction theory with $g_2 = g_B$ of equation (14*a*) due to the screened range.

We have seen that the screened range may produce factorials additional to those which enter in the definition of the diagram itself, i.e. which appear in the constant-interaction theory. In principle the additional factorials may either introduce a qualitative change in the result (38*b*), i.e. the asymptotic behaviours faster than that, or produce less important « quantitative » changes of the result (38*b*).

Fig. 8. — Correlation function ladder diagram $\hat{L}^{(p)}$.

Let us thus start by examining the ladder diagrams in which the additional factorials appear already in the second order. In the evaluation of ladder diagrams it is somewhat more convenient to consider the correlation function diagrams instead of the triangular diagrams of figures 2 and 6. An example of such a diagram is shown in figure 8. The low order diagrams of this kind are obtained by closing the external lines in figures 2 and 6, and we shall denote them by $\hat{M}$ and $\hat{L}$. This step allows us to draw a simple consequence from the $|\Omega_2|$ dependence of the contributions (21), (29) and (30). M_S, L_{BS} and L_{SS} are coupled to the logarithmic integration over

$| \Omega_2 |$ in contrast to M_B, L_{BB} and L_{SB} of equations (23*a*), (28) and (31). Thus, in the $\omega_0 \lesssim \varepsilon_F$ limit, we have

$$\hat{M}_B = g_B \log^2 \frac{\varepsilon_F}{| \Omega |}$$
$$\hat{M}_S = \frac{1}{2!} g_S \log^2 \frac{\varepsilon_F}{| \Omega |}, \tag{39}$$

and

$$\hat{L}_{BB} = g_B^2 \log^2 \frac{\varepsilon_F}{| \Omega |},$$
$$\hat{L}_{SB} = \hat{L}_{BS} = \frac{1}{2!} g_B g_S \log^2 \frac{\varepsilon_F}{| \Omega |}, \tag{40}$$
$$\hat{L}_{SS} = \frac{1}{3!} g_S^2 \log^3 \frac{\varepsilon_F}{| \Omega |}.$$

A brief thinking based on the discussion below equation (29) shows that the factorial in (39) and (40) is equal to $(v + 1)$!, where v is the number of neighbouring g_S's which couple the logarithmic integrations.

This result can be readily extended to the p-th order ladder diagram of figure (8). Each line in this diagram should be understood to represent either g_S or g_B, analogously to the separation in equations (39) and (40). Furthermore, we have to focus our attention on the chains of the neighbouring g_S's, since each such chain of the length v produces $(v + 1)$! in the denominator. The theory of runs [23] tells us that out of $\binom{p}{r}$ configurations with r g_S-lines and $p - r$ g_B-lines,

$$\frac{k!}{k_1! \ldots k_v! \ldots k_r!} \binom{p - r + 1}{k}$$

are built of k_1 g_S-chains of unit length, ..., k_v g_S-chains of length v, so that $k = \sum_{v=1}^{r} k_v$, $r = \sum_{v=1}^{r} v k_v$. All these configurations are associated with the same prefactor coming from the coupling of the logarithmic integrations,

$$\frac{1}{(1 + 1)!^{k_1} \ldots (v + 1)!^{k_v} \ldots (r + 1)!^{k_r}}$$

The p-th order diagram can be therefore written as

$$\hat{L}^{(p)} \simeq \log^{p+1} \frac{\varepsilon_F}{| \Omega |} \sum_{r=0}^{p} g_B^{p-r} g_S^r \sum_{k=1}^{r+1} \binom{p - r + 1}{k} \times$$
$$\times \sum_{\substack{k_1 \ldots k_r \\ \Sigma v k_v = r \\ \Sigma k_v = k}} \frac{1}{(1 + 1)!^{k_1} \ldots (v + 1)!^{k_v} \ldots (r + 1)!^{k_r}} \frac{k!}{k_1! \ldots k_v! \ldots k_r!}. \tag{41}$$

We shall further note that the expression for $\hat{L}^{(p)}$ obtained by a minorization $(1 + v)^{k_v} \approx 1$ differs from that with a majorization $(1 + v)^{k_v} \approx e^{v k_v}$ by replacing g_S by g_S/e, since $e^{\Sigma v k_v} = e^r$. Neglecting this renormalization of g_S, between e and unity, unimportant for our qualitative purposes, we shall approximate $(v + 1)!^{k_v}$ in equation (41) by $v!^{k_v}$. The sum over $k_1 \ldots k_v \ldots k_r$ can then be recognized as a definition of the Stirling numbers [24]. Using the sum rules [24] obeyed by these numbers we find that

$$\hat{L}^{(p)} \approx \log^{p+1} \frac{\varepsilon_F}{| \Omega |} \sum_{r=0}^{p} \frac{(p - r + 1)^r}{r!} g_B^{p-r} g_S^r. \tag{42}$$

The combinatorial factor in (42) replaces $\binom{p}{r}$ which would occur if the coupling of the logarithmic integrations were not present, i.e. if the bare and screened range were acting additively. In order to see whether this difference leads to the qualitatively new behaviour of $\hat{L}^{(p)}$ with respect to the constant-interaction case we must evaluate $\hat{L}^{(p)}$ for large p. This can be done by the saddle point approximation, i.e. through the largest term of (42). The latter is determined as a solution of

$$(1 - y) \log \left(\frac{1}{y} - 1 \right) = 1 - (1 - y) \log x \tag{43}$$

where $y = r/p$, $x = g_S/g_B$ and we have used the Stirling approximation for the factorials. In figure 9 we plot the graphical solution of equation (43) $y = y(x)$, as well as the coefficient a appearing in

$$\hat{L}^{(p)} \simeq (a g_B)^p \log^{p+1} \frac{\varepsilon_F}{| \Omega |}$$
$$a(x, y(x)) = \left(\frac{1}{y} - 1 \right)^y x^y. \tag{44}$$

In the whole range $0 < g_S/g_B < 10$, a is of the order of unity, i.e. the contribution of the screening range to $\hat{L}^{(p)}$ is practically negligible. The asymptotic behaviour of the ladder series (42) is therefore geometric as in the $\omega_0 \ll \varepsilon_F$ case of the preceding section. Only for the unphysical values of x, $x > 10$ the radius of convergence of the ladder series in terms of $g_S^p \log^{p+1} \varepsilon_F/| \Omega |$ (note g_S instead of g_B) starts increasing. As easily seen directly from equation (42) it becomes infinite for $g_B = 0$, when $\hat{L}^{(p)}$ becomes a term of the exponential expansion. In conclusion the additional factorials do not produce qualitative changes of the asymptotic ladder diagram in the interesting $g_B \approx g_S$ regime. The ladder diagram series remains geometric and determined by g_B, i.e. it is the same as in the $\omega_0 \lesssim \varepsilon_F$ limit of our $\omega_0 \ll \varepsilon_F$ approximation.

Unfortunately we can not extend this conclusion

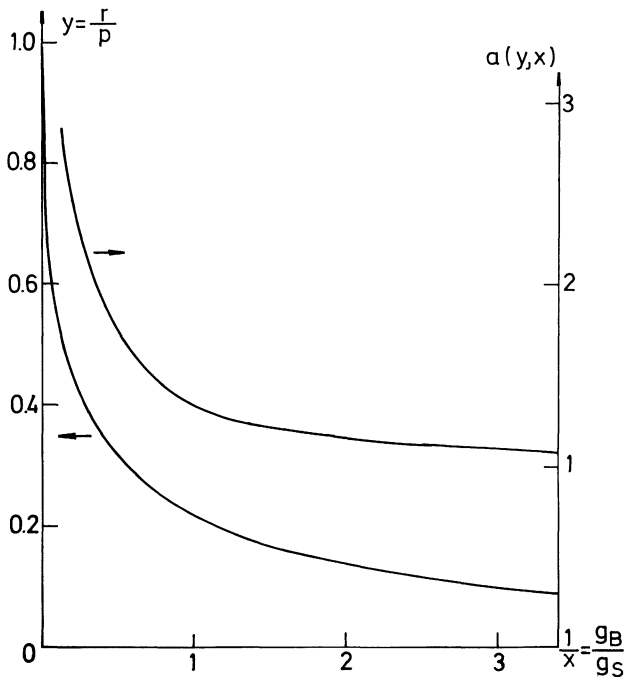

Fig. 9. — Value of r which gives dominant contribution to the p-th order ladder diagrams as a function of g_B/g_S. Corresponding value of a prefactor a multiplying the coupling constant g_B in the correlation function ladder diagram.

straightforwardly to the whole parquet because the additional factorials do not appear symmetrically in the denominators of all parquet diagrams. E.g. we concluded that they do not appear in the second order in the diagrams of the N-type. Equation (34) was even written in the form which suggests that the factorials may appear in the numerator of the high-order N-type diagrams of figure 10. This however can be ruled out by a closer examination of these diagrams : factorials in the numerator would require the accumulation of many angular interactions v_s in the same angular integration. Contrary to that, the interactions join two by two in the high-order N-type diagrams. This leads to the powers of c rather then to the factorials in the numerator. If we ignore the difference between the quantities such as cv^2 of (34) and g_S^2 of (20) we can say that in these diagrams the bare and screened ranges act more additively than in the ladder diagrams, i.e. their effective coupling constant is close to $g_B + g_S$. Presumably, the general parquet diagram falls between the two extremes fixed by the ladder and N-type diagrams, i.e. its effective coupling constant is somewhere between g_B and $g_B + g_S$. The variations of the effective coupling constant from one to another

Fig. 10. — High-order mixed diagram (no ladder inserts).

parquet diagram are sizeable i.e. of the order of $g_S \approx g_B$, but the qualitative changes such as that in the ladder diagram $\hat{L}^{(p)}$ at $g_B = 0$ are not expected. It is even reasonable to expect that in the *average* parquet diagram the role of the screened range is diminished by the additional factorials and that the straightforward $\omega_0 \lesssim \varepsilon_F$ limit of our $\omega_0 \ll \varepsilon_F$ theory is roughly correct.

8. **Concluding remarks.** — There is no conceptual difficulty to extend the results of the two preceding sections to the case with backward scattering. The elementary square diagrams involving only g_1 of equation (4) satisfy the requirements of the single variable parquet theory and so do the cross-terms $g_1 M$ and $g_1 C$ of equation (16). The conditions of the validity of the single variable theory remain therefore the same as for the corresponding Tomonaga model.

New many-body effects occur in the limit $\log \varepsilon_F/\omega_0 > v^{-1/2}$ of the loosely packed chains when the degeneracy of the diagrams with the same number of integrations is lifted at high frequencies due to the long-range nature of the forward interaction

$$g_2 = u_B(|\Omega|) + g_B(|\Omega|) \qquad (45)$$

given by equations (13) and (14). This represents the generalization of the result (38a). Postponing the discussion of these effects to a separate paper we shall briefly mention here the two more conventional situations when the $|\Omega|$ structure of g_2 is unimportant.

The first corresponds to the case when $|u_B| > g_B$. This is the (extended) Hubbard Hamiltonian limit. In this limit it is convenient to include the short-range forces of the non-Coulombian origin into the difference between u_B and u of equation (4).

The second simple situation corresponds to the $\log \varepsilon_F/\omega_0 < v^{-1/2}$ limit of the closely packed chains encountered in section 6. The conventional parquet results in terms of $g_2 - g_1/2$, hold then in the whole singular regime. Moreover our theory provides the explicit expressions (4) and (45) for g_1 and g_2. If we assume that u is of the Coulomb origin, $g_2 - g_1/2$ tends to be positive. The tendency to the charge density wave, associated with the Madelung energy in the second term of $g_1^{\parallel}$ in (4), is increased by the $\log \varepsilon_F/\omega_0$ enhancement of g_B over the first-neighbour Coulomb interaction v. This indicates that the appearance of superconductivity requires the mechanism additional to the Coulomb interaction. It is however important that the repulsive long-range forces contribute to g_2 a term $g_B < 1$ which can be overcome by the short-range phonon mediated attraction. This result is due to the dynamic screening which led to $g_S < g_B < 1$ i.e. to the dominant role of g_B. In this sense we can say that the superconductivity is due to the combined activity of plasmons and phonons.

These considerations explain the qualitative success of the constant-interaction theory in accounting for the phase diagrams of real systems exhibiting superconductivity, although the present analysis indicates that they belong to the intermediate $\omega_0 \approx \varepsilon_F$ or even the $\omega_0 > \varepsilon_F$ strong coupling regime. The investigation of the strong coupling limit of our problem would be certainly clarifying in this sense. However, it should use the methods [4] completely different from those employed here.

Acknowledgments. — I benefited from the discussions with L. P. Gor'kov, J. Friedel, Ph. Nozières and S. A. Brazovskii. A. Bjeliš kindly read the manuscript. Some early stages of the work were performed at the Laboratoire de Physique des Solides, Orsay and International Centre for Theoretical Physics, Trieste.

Appendix. — The diagram N of figure (7) contains four electron propagators. With external variables set equal to zero their product is

$$GGGG = \frac{-\,\mathrm{e}^{-i(\phi_1-\phi_2)}}{\rho_1\,\rho_2\,|\,\rho_1^2+\rho_2^2-2\,\rho_1\,\rho_2\cos(\phi_1-\phi_2)\,|} \tag{A.1}$$

written in terms of the amplitudes and phases of the interaction variables. To fix the ideas let us discuss N_{SS}. The interactions are therefore given by equation (19),

$$N_{SS} = \frac{(-1)}{4\,\pi^2}\int \frac{\mathrm{e}^{-i(\phi_1-\phi_2)}\,v(\phi_1)\,v(\phi_2)}{\rho_1^2+\rho_2^2-2\,\rho_1\,\rho_2\cos(\phi_1-\phi_2)}\,\mathrm{d}\rho_1\,\mathrm{d}\rho_2\,\mathrm{d}\phi_1\,\mathrm{d}\phi_2\,. \tag{A.2}$$

The first logarithmic singularity can be extracted from the two radial integrations by going to the polar variables r, θ in the ρ_1, ρ_2 space. The r-integration gives a logarithmically singular factor, whereas the remaining integration reads

$$J(\phi) = \int_0^{\pi/2} \frac{\mathrm{d}\theta}{1-\cos\phi\,\sin 2\,\theta}, \tag{A.3}$$

where we have abbreviated $\phi_1 - \phi_2$ by ϕ. The result of the integration (A.3) depends on the quadrants to which ϕ_1 and ϕ_2 belong. With ϕ_1 and ϕ_2 both in the first quadrant, $|\,\phi\,| < \pi/2$, and

$$J_{11}(\phi) = \frac{\pi - |\,\phi\,|}{|\sin\phi\,|}. \tag{A.4}$$

Similarly, for ϕ_1 in the first quadrant and ϕ_2 in the third, $\phi_2 = \pi + \tilde{\phi}_2$, we have

$$J_{13}(\phi) = \frac{|\,\tilde{\phi}\,|}{|\sin\tilde{\phi}\,|}, \tag{A.5}$$

where $\tilde{\phi} = \tilde{\phi}_1 - \tilde{\phi}_2 = \phi + \pi$ (i.e. $\tilde{\phi}_1 = \phi_1$) and $|\,\tilde{\phi}\,| < \pi/2$. The shift to the new variables leaves the interactions in equation (A.2) invariant but changes $\mathrm{e}^{-i\phi}$ into $-\,\mathrm{e}^{-i\tilde{\phi}}$.

In this way we get

$$N_{SS}^{(11)} + N_{SS}^{(13)} = -\frac{1}{4\,\pi^2}\int_0^{\omega_0}\frac{\mathrm{d}r}{r}\int_0^{\pi/2}\int_0^{\pi/2}\frac{\pi - 2\,|\,\phi\,|}{|\sin\phi\,|}\,v_s(\phi_1)\,v_s(\phi_2)\,\mathrm{e}^{-i\phi}\,\mathrm{d}\phi_1\,\mathrm{d}\phi_2\,. \tag{A.6}$$

The main singularity in the angular part of equation (A.6) is $|\sin\phi\,|^{-1}$, which falls on the bissectrix of the integration range. The similar procedure casts $N_{SS}^{(12)} + N_{SS}^{(14)}$ into the form analogous to (A.6), such that $2\,|\,\phi\,|$ is replaced by $2\,\phi$ and $\phi = \phi_1 + \phi_2$. This latter means that the singularity of $|\sin\phi\,|^{-1}$ is not contained in the integration range and the four contributions of this kind can be discarded. Collecting then those of the type (A.6) we get $N \approx 4(N_{SS}^{(11)} + N_{SS}^{(13)})$, i.e. equation (33) of section 5.

References

[1] JÉROME, D., MAZAUD, A., RIBAULT, M., *J. Physique Lett.* **41** (1980) 95. For a summary of recent experimental results see *Proceedings of the International Conferences on Low-Dimensional Conductors*, Boulder, 1981.

[2] BYCHKOV, YU. A., GOR'KOV, L. P., DZYALOSHINSKII, I. E., *Zh. Eksp. Teor. Fiz.* **50** (1966) 738 [*Sov. Phys. JETP* **23** (1966) 489].

[3] SÓLYOM, J., *Adv. Phys.* **28** (1979) 201 — review with all but the most recent references.

[4] EMERY, V. J., review in *Highly Conducting One-Dimensional Solids*, edited by J. T. Devreese, R. P. Evrard and V. E. van Doren (Plenum, New York) 1979.

[5] PRIGODIN, V. N., FIRSOV, Yu., *Zh. Eksp. Teor. Fiz.* **76** (1979) 1602 [*Sov. Phys.-JETP* **49** (1979) 813].

[6] LABBÉ, J., FRIEDEL, J., *J. Physique* **27** (1966) 153 and 303 ;
LABBÉ, J., BARIŠIĆ, S., FRIEDEL, J., *Phys. Rev. Lett.* **19** (1968) 1038.

[7] For an updated version of the mean-field results see HOROWITZ, B., GUTFREUND, H., WEGER, M., *Solid State Commun.* **39** (1981) 541.

[8] GOR'KOV, L. P., *Proceedings of the International Conference on Quasi One-Dimensional Conductors*, Dubrovnik 1978, Edited by S. Barišić, A. Bjeliš, J. R. Cooper and B. Leontić in *Lecture Notes in Physics* **96** (1979) 1 (Springer Verlag) and *Letters to Zh. Eksp. Teor. Phys.* **34** (1981) 602.

[9] BARIŠIĆ, S., BRAZOVSKII, S. A., in *Recent Developments in Condensed Matter Physics*, edited by J. T. Devreese (Plenum, New York) vol. 1, 1981, p. 327.

[10] EMERY, V. J., BRUINSMA, R., BARIŠIĆ, S., *Phys. Rev. Lett.* **48** (1982) 1039.

[11] BARIŠIĆ, S., *Phys. Rev. B* **5** (1972) 932 and 941.

[12] BRUESCH, P., *Proceedings of the International Conference on One-Dimensional Conductors*, Saarbrucken 1974 ; *Lecture Notes in Physics* **34** (1975) (Springer Verlag) ;
TANNER, D. B., JACOBSEN, C. S., GARITO, A. F., HEEGER, A. J., *Phys. Rev. B* **13** (1976) 3381 ;
JACOBSEN, C. D., TANNER, D. B., BECHGAARD, K., *Phys. Rev. Lett.* **46** (1981) 1142 ; some data are compiled in Ref. [9].

[13] DZYALOSHINSKII, I. E., LARKIN, A. Y., *Zh. Eksp. Teor. Fiz.* **65** (1973) 411 [*Sov. Phys. JETP* **38** (1974) 202].

[14] ŠAUB, K., BARIŠIĆ, S., FRIEDEL, J., *Phys. Lett. A* **56** (1976) 302.

[15] HARTZSTEIN, C., ZEVIN, V., WEGER, M., *J. Physique* **41** (1980) 677.

[16] DZYALOSHINSKII, I. E., KATS, E. I., *Z. Eksp. Teor. Fiz.* **55** (1968) 338 [*Sov. Phys. JETP* **28** (1969) 178] ;
WILLIAMS, P. F., BLOCH, A. N., *Phys. Rev. B* **10** (1974) 1097.

[17] DZYALOSHINSKII, I. E., LARKIN, A. Y., *Zh. Eksp. Teor. Fiz.* **61** (1971) 791.

[18] ROULET, B., GAVORET, J., NOZIERES, P., *Phys. Rev.* **178** (1969) 1972 and references therein.

[19] GOR'KOV, L. P., DZYALOSHINSKII, I. E., *Zh. Eksp. Teor. Fiz.* **67** (1974) 397 [*Sov. Phys. JETP* **40** (1975) 1980].

[20] KLEMM, R. A., GUTFREUND, H., *Phys. Rev. B* **14** (1976) 1086.
For a classical analogue of this argument see : BATISTIĆ, I., THEODOROU, G., BARIŠIĆ, S., *J. Phys. C* **14** (1981) 1905.

[21] MIHÁLY, L., SÓLYOM, J., *J. Low Temp. Phys.* **24** (1976) 579 ;
MENYHARD, N., *Lecture Notes on Physics*, Vol. 65, Edited by L. Pál, G. Grüner, A. Jánossy and J. Sólyom, (Springer Verlag) Berlin.

[22] BOTRIĆ, S., BARIŠIĆ, S., to be published.

[23] FELLER, W., *An Introduction to Probability Theory and Its Applications*, Vol. 1, (J. Wiley & Sons, Inc.) 1968, p. 62.

[24] SAČKOV, V. N., *Combinatorial Methods of the Discrete Mathematics* (in Russian) (Nauka, Moscow) 1977 ; see also *Handbook of Mathematical Functions*, Edited by M. Abramovitz, I. E. Stegun (Dover Publications, Inc. N. Y.).